Journal of Hazardous Materials 504 (2026) 141380

Contents lists available at ScienceDirect

Journal of Hazardous Materials

journal homepage: www.elsevier.com/locate/jhazmat

Non-targeted screening of alprazolam and flualprazolam metabolites in *in vitro* metabolism of different species by high-resolution mass spectrometry

Jinxia Dai [a], Hui Lin [b], Jun-qin Qiao [a], Hong-zhen Lian [a,*], Chun-xiang Xu [b,*]

[a] State Key Laboratory of Analytical Chemistry for Life Science, School of Chemistry & Chemical Engineering and Center of Materials Analysis, Nanjing University, Nanjing 210023, China
[b] Jiangsu Institute for Food and Drug Control, Nanjing 210008, China

HIGHLIGHTS

- *In vitro* phase I and II metabolism of ALP and FALP was profiled.
- Eleven metabolites were identified for each drug using HRMS non-targeted screening.
- Discovered new hydroxylation sites on benzene ring and corresponding metabolites.
- Distinct interspecies metabolic patterns revealed differences in residue markers.
- *In-silico* toxicity prediction indicated potential environmental and biological risks.

GRAPHICAL ABSTRACT

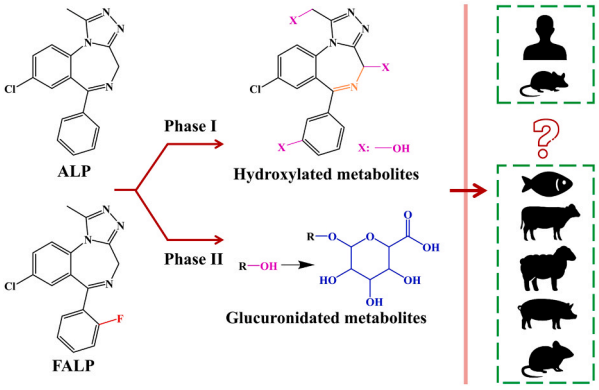

ARTICLE INFO

Keywords:
Alprazolam
Flualprazolam
Metabolic transformation
Non-targeted screening
Species differences

ABSTRACT

Flualprazolam (FALP), a new psychoactive benzodiazepine structurally related to alprazolam (ALP), is increasingly misused, yet its interspecies metabolism remains unclear. In this study, the *in vitro* phase I and II metabolism of ALP and FALP was systematically investigated across multiple species under optimized liver microsome incubation conditions (1.5 mg mL^{-1}, 2 h), using a non-targeted screening strategy with high-resolution mass spectrometry (HRMS). ALP and FALP exhibited similar metabolic profiles, with 11 metabolites each, including 7 phase I and 4 phase II metabolites, of which 6 were newly discovered. Species-specific differences were observed, with humans and mice primarily producing 4- and α-hydroxylated metabolites, while edible animals such as fish, bovine, sheep, and pig mainly generated 4-hydroxylated metabolites. This interspecies discrepancy suggests that the currently designated residue markers for ALP in animal-derived foods may not accurately reflect its actual metabolic fate. Notably, newly identified benzene-ring hydroxylated metabolites were more abundant in rats and livestock, and toxicity predictions indicated that these metabolites, including M1, M5, and M7, may pose higher ecotoxicological or developmental risks than the parent drugs, with greater predicted toxicity than the α-hydroxylated metabolites currently used as residue markers. These findings provide detailed insights into

* Corresponding authors.
E-mail addresses: hzlian@nju.edu.cn (H.-z. Lian), xcx70@163.com (C.-x. Xu).

https://doi.org/10.1016/j.jhazmat.2026.141380
Received 23 October 2025; Received in revised form 19 January 2026; Accepted 3 February 2026
Available online 4 February 2026

interspecies metabolic patterns, emphasize the need to consider species-specific metabolites in residue monitoring, and inform the toxicological assessment of benzodiazepines in food and environmental contexts.

1. Introduction

Benzodiazepines are widely used psychotropic drugs in both human and veterinary medicine for their anxiolytic, hypnotic, anticonvulsant, and sedative effects [1–3]. However, owing to their adverse effects on the central nervous system of humans, benzodiazepines are subject to strict regulation or prohibition in many countries and organizations. Despite this, misuse and illegal application remain prevalent [4], including their illicit addition to alcoholic beverages and unauthorized use in animal husbandry or aquaculture [5–7]. As a result, the parent drugs and metabolites inevitably remain in animal-derived foods, causing potential risks to animal and human health [8]. In addition, drugs and their metabolites can enter urban wastewater after humans excretion and ultimately accumulation in aquatic organisms [9–11].

In recent years, the emergence of new psychoactive substances has further complicated regulatory control and risk assessment [12]. Among these, new benzodiazepine analogues have gained increasing attention due to their structural similarity to approved drugs and comparable pharmacological effects, despite lacking formal approval and toxicological evaluation [13–15]. Flualprazolam (FALP) is a representative example of this class and is a fluorinated analogue for the common and strictly controlled benzodiazepine drug alprazolam (ALP) [16,17], and its chemical structural formula is shown in Fig. 1. Since its first seized by police in Sweden in November 2017, FALP has been increasingly reported in some international drug seizures, clinical and autopsy cases worldwide, prompting regulatory control in multiple countries [18–20]. In 2021, China officially included FALP in the list of non-medicinal narcotics and psychotropic substances [21]. These reports highlight the growing prevalence of FALP in both illicit and regulatory contexts, underscoring the need to investigate its metabolic fate in humans and animals.

The metabolism of benzodiazepines plays a critical role in determining their pharmacological activity, toxicity, and residue characteristics. The metabolism of ALP has been relatively well investigated, with hydroxylated products, such as α-hydroxy alprazolam (α-OHALP), 4-hydroxy alprazolam (4-OHALP) and α,4-dihydroxy alprazolam (α,4-dihydroxy-ALP) identified as major phase I products [22,23]. In 2019, α-OHALP, a metabolite of ALP, was listed for the first time in the standard method for the detection of benzodiazepines in foodstuffs for export from China [24]. In contrast, studies on FALP metabolism remain limited. Available reports have primarily focused on *in vitro* human-derived systems or single model animal, with limited metabolite coverage and inconsistent findings [25,26]. Importantly, there is currently a lack of more research on the metabolism of FALP in edible animals and aquatic species.

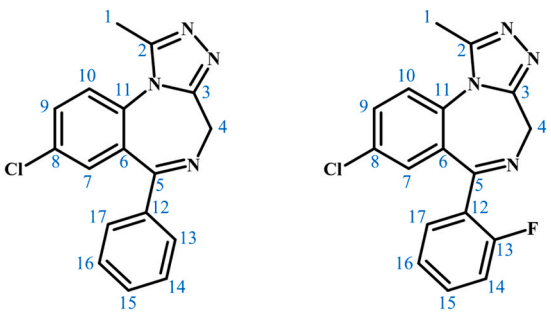

Fig. 1. Structural formula of ALP and FALP.

Drug metabolism is known to exhibit pronounced interspecies differences, mainly driven by variability in cytochrome P450 enzyme systems [27,28]. Metabolic differences among species may result in distinct metabolic pathways and residual markers of drugs in humans and animals, leading to erroneous evaluations of human drugs for veterinary use. Previous metabolism studies of benzodiazepines have predominantly focused on humans and model animals, whereas comparative interspecies metabolism across aquatic organisms and livestock has received limited attention. From a methodological perspective, most existing studies rely on targeted analytical strategies, which inherently restrict the identification of unexpected or new metabolites. High-resolution mass spectrometry (HRMS) offers a powerful platform for comprehensive metabolite profiling, enabling the detection and structural elucidation of both known and unknown transformation products [29]. In addition, *in vitro* metabolism provides a controllable and reproducible platform for comparing metabolic behaviors across multiple species. Compared with *in vivo* metabolism, it has the advantages of easy control of metabolic conditions and simple experimental operations [30–32]. However, despite these capabilities, its application as a unified non-targeted HRMS workflow to systematically and comparatively investigate both phase I and phase II metabolism of benzodiazepines across diverse species remains largely unexplored.

The primary objectives of this study were to identify new and previously unreported metabolites of ALP and FALP generated across different species, and to compare interspecies metabolic pathways in order to reveal species-specific biotransformation characteristics relevant to toxicological evaluation and the selection of residue markers. Therefore, this work systematically investigated the phase I and II *in vitro* metabolism of FALP using ultrahigh-performance liquid chromatography coupled with quadrupole Orbitrap mass spectrometry (UHPLC-Q-Orbitrap MS), with ALP included as a reference compound to elucidate the metabolism rules of benzodiazepines. The *in vitro* metabolism differences of ALP and FALP were comparatively evaluated across multiple species, including humans, model animals (rat and mouse), aquatic animals (fish), and livestock animals (bovine, sheep, and pig). In addition, *in-silico* toxicity predictions were conducted for both parent compounds and their identified metabolites. The results provide valuable insight into the interspecies metabolic transformation of new psychoactive benzodiazepines and offer a scientific basis for the monitoring and risk assessment of their residues in environmental and food safety contexts.

2. Materials and methods

2.1. Chemical and reagents

ALP and FALP were purchased from Shanghai Yuansi Standard Science and Technology Co., Ltd. (Shanghai, China). α-OHALP and α-OHFALP were purchased from Alexis (Lausen, Switzerland) and Glpbio (Montclair, CAL, USA) respectively. Acetonitrile and methanol, HPLC-MS grade, were obtained from Sigma-Aldrich (Darmstadt, Germany). PBS buffer (0.1 M, pH 7.2) was obtained from Shanghai Yuanye Bio-Technology Co., Ltd. (Shanghai, China). Nicotinamide adenine dinucleotide phosphate (NADPH) regeneration system solution and uridine diphosphate glycosyltransferase (UGT) incubation system solution were purchased from Beijing Huizhi Heyuan Biotechnology Co., Ltd. (Beijing, China). The NADPH regeneration system solution consisted of solution A (26.1 mM $NADP^+$, 66 mM glucose 6-phosphate, 66 mM magnesium chloride) and solution B (40 U mL^{-1} glucose 6-phosphate dehydrogenase, 5 mM sodium citrate). The UGT incubation system solution consisted of 250 μg mL^{-1} alamethicin, 50 mM uridine

diphosphate glucuronic acid (UDPGA), and 50 mM D-glucaric acid-1,4-lactone. Human, rat, mouse, fish, bovine, sheep, and pig liver microsomes were supplied by Qishi Biotechnology Co., Ltd. (Shanghai, China) at an enzyme concentration of 20 mg mL^{-1} and stored at −80 °C. A Millipore Milli-Q plus ultrapure water system (Milford, MA, USA) was used to provide ultrapure water.

2.2. Preparation of standard solution

The solid standards of ALP, FALP, α-OHALP and α-OHFALP were respectively dissolved in methanol to prepare 10 mg mL^{-1} (ALP and FALP) and 1 mg mL^{-1} (α-OHALP and α-OHFALP) stock standard solutions. Individual standard working solutions were prepared at 100 mg L^{-1} by diluting the stock standard solutions with acetonitrile. All the stock standard solutions and standard working solutions were kept at −20 °C in brown glass bottles. The standard working solutions were serially diluted with acetonitrile/PBS solution (*v/v*, 1:1) to prepare mixed solutions of 1, 2, 5, 10, 20, 50, 100 and 200 μg L^{-1}, which were used to prepare calibration curves for quantitative analysis.

2.3. Sample preparation

2.3.1. Sample preparation for phase I in vitro metabolism

First, 28 μL of PBS solution, 10 μL of solution A and 2 μL of solution B of the NADPH regeneration system solution were added to a 1.5 mL centrifuge tube, and vortexed for 1 min. Then, the mixed solution was pre-incubated in a 37 °C water bath for 5 min, and 15 μL of 20 mg mL^{-1} liver microsomes, 144 μL of PBS solution and 1 μL of 10 mg mL^{-1} ALP or FALP solution were added sequentially, and vortexed for 1 min. The final incubation volume was 200 μL, resulting in a final organic solvent (methanol) content of approximately 0.5 % (*v/v*), as determined by volumetric calculation, a level widely considered non-inhibitory to microsomal enzyme activity. After the mixture was incubated in a 37 °C water bath for 2 h, 200 μL of ice-cold acetonitrile (pre-cooled at −20 °C) was added to terminate the reaction to inactivate microsomal enzymes. The reactant mixture was vortexed for 1 min and centrifuged at 13,000 rpm for 5 min. Finally, the supernatant was filtered through a 0.22 μm organic phase membrane filter into a sample vial for UHPLC-Q-Orbitrap MS analysis.

2.3.2. Sample preparation for phase II in vitro metabolism

First, 10 μL of solution A and 2 μL of solution B of the NADPH regeneration system solution, 20 μL of 250 μg mL^{-1} alamethicin, 20 μL of 50 mM UDPGA, 20 μL of 50 mM D-glucaric acid-1,4-lactone and 112 μL of PBS solution were added to a 1.5 mL centrifuge tube, and vortexed for 1 min. Then, the mixed solution was pre-incubated in a 37 °C water bath for 5 min, and 15 μL of 20 mg mL^{-1} liver microsomes and 1 μL of 10 mg mL^{-1} ALP or FALP solution were added sequentially, and vortexed for 1 min. The final volume was 200 μL, with the organic solvent content calculated to keep below 1 % (*v/v*). After incubating the mixed solution in a 37 °C water bath for 2 h, 200 μL of ice-cold acetonitrile (pre-cooled at −20 °C) was added to inactivate enzymes and terminate the reaction. The reactant mixture was vortexed for 1 min and centrifuged at 13,000 rpm for 5 min. Finally, the supernatant was filtered through a 0.22 μm organic phase membrane filter into a sample vial for UHPLC-Q-Orbitrap MS analysis.

2.4. Instrument conditions

Liquid chromatography was performed on an Ultimate 3000 UHPLC system (Thermo Fisher Scientific, San Jose, CA, USA). A ZORBAX RRHD SB C18 column (100 mm × 2.1 mm, 1.8 μm, Agilent, USA) was used for the separation of analytes, and the column temperature was set at 40 °C. The mobile phase consisted of eluent A (0.1 % *v/v* formic acid in water) and eluent B (acetonitrile). The gradient elution was as follows: 0–2 min, 90 % A; 2–15 min, 90 %-20 % A; 15–16 min, 20 % A; 16–17 min, 20 %-90 % A; 17–18 min, 90 % A. The flow rate of the mobile phase was 0.3 mL min^{-1}, and the injection volume was 5 μL.

A Q-Exactive quadrupole-Orbitrap mass spectrometer (Thermo Fisher Scientific, Bremen, Germany) was equipped with an electrospray ionization (ESI) source in positive ionization mode. The parameters of mass spectrometer were set as follows: sheath gas (N_2, > 99 %), 40 arbitrary units (arb); auxiliary gas (N_2, > 99 %), 10 arb; spray voltage, 3.5 kV; capillary temperature, 320 °C; vaporizer temperature, 350 °C; S-lens voltage, 60 %; scan mode, Full MS/dd-MS^2 (resolution 70,000/17,500 FWHM); scan range, *m/z* 50–750; normalized collision energy (NCE), 20, 40, 50; loop count, 10; MSX count, 1; dynamic exclusion time, 2 s. The maximum injection time and AGC target were set to default values, 100 ms/$3e^6$ and 50 ms/$1e^5$ corresponding to Full MS and dd-MS^2 respectively.

2.5. Data analysis

The following software was used: Xcalibur™ 3.1, Qual Browser, Quan Browser, Compound Discoverer 3.1, Mass Frontier 7.0 (Thermo Fisher Scientific, Waltham, MA, USA), and CFM-ID 2.4. Raw data were acquired and processed using Xcalibur, and Qual Browser and Quan Browser were used for qualitative and quantitative analysis of ALP, FALP and their metabolites. Raw data files were imported into Compound Discoverer for non-targeted metabolite screening and identification. Non-targeted data processing was conducted using the workflow template "MetID w Stats Expected and Unknown w Background Removal" (Figure S1). The workflow involved spectral alignment, compound detection and grouping, metabolite prediction, and blank-based background subtraction, followed by database searching against mzCloud and ChemSpider with FISh scoring applied to improve MS/MS-based metabolite identification confidence. Compound identification was performed using high-confidence criteria, including a precursor ion mass error ≤ 5 ppm and fragment ion mass error ≤ 10 ppm. Structural elucidation and fragmentation interpretation were further assisted by Mass Frontier and CFM-ID, enabling rational confirmation of proposed metabolite structures.

2.6. Toxicity prediction

The *in-silico* prediction of drug toxicity was performed through the following tools: ECOSAR software (Ecological Structure-Activity Relationship v1.11) for predicting ecotoxicity and TEST software (Toxicity Estimation Software Tool v5.1.2) for predicting ecotoxicity and developmental toxicity.

3. Results and discussion

3.1. Optimization of LC-MS conditions

To preliminarily obtain the *in vitro* metabolites of ALP and FALP for optimizing subsequent experimental conditions, the preliminary experiment was conducted under the following *in vitro* incubation conditions: rat liver microsome concentration of 0.5 mg mL^{-1}, drug concentration of 0.5 mg L^{-1}, and incubation time of 4 h. Different metabolites have similar chemical structure to their parent drug and are usually difficult to separate on chromatography, especially for isomers, which impacts the identification and quantification of the metabolites. In order to better retain and separate different metabolites, the LC conditions of the instrumentation were optimized. The sample obtained after FALP incubation was analyzed using the mobile phase gradient shown in Figure S2**-a**, and multiple chromatographic peaks were observed in the extracted ion chromatogram of α-OHFALP (*m/z* 343.0756), corresponding to multiple isomers. Comparing with the α-OHFALP standard solution, the chromatographic peak of α-OHFALP overlapped with that of another isomer metabolite, and the retention times (t_R) were 7.43 and 7.34 min respectively, as shown in Figure S3.

This isomer was initially identified as 4-OHFALP, and its detailed identification analysis was shown in the subsequent discussion section. After trying to change the mobile phase gradient (Figure S2-**b**), it was still difficult to achieve good separation between α-OHFALP and 4-OHFALP, as shown in the two chromatographic peaks corresponding to 1 and 2 in Fig. 2-**a**. Different C18 chromatographic columns generally have different side chain groups, which can lead to differences in separation. Therefore, four different C18 reversed-phase chromatographic columns were selected for comparison to examine their separation capabilities of metabolites. The Eclipse Plus C18 column (100 mm × 2.1 mm, 1.8 μm, Agilent, USA), ACUITY UPLC® BEH C18 column (100 mm × 2.1 mm, 1.7 μm, Waters, USA), Hypersil GOLD C18 column (100 mm × 2.1 mm, 3 μm, Thermo, USA) and ZORBAX RRHD SB C18 column (100 mm × 2.1 mm, 1.8 μm, Agilent, USA) were tested in this study. The separation effects of α-OHFALP and 4-OHFALP were compared, and ZORBAX RRHD SB C18 column was selected as the separation column, which had the best selectivity and separation effect, as shown in Fig. 2-**d**. When the glucuronidated metabolites produced by phase II metabolism were analyzed under this chromatographic condition, it was found that the extracted ion chromatographic peaks of *m/z* 519.1077 and *m/z* 522.1074 had poor peak shape. Therefore, on the basis of using this chromatographic column for separation, the mobile phase condition of gradient 3 (Figure S2-**c**) was selected, and by reducing the proportion of the initial acetonitrile phase, better chromatographic peak shape and sensitivity were obtained, as shown in Figure S4.

In order to obtain rich MS^2 fragmentation information, taking the phase I metabolite (*m/z* 343.0756) and phase II metabolite (*m/z* 522.1074) of FALP as examples, the MS^2 spectra corresponding to different NCEs (20, 30, 40, 50, 60) were investigated, as shown in Figure S5. The evaluation of fragment ion coverage and abundance across different NCEs showed that the optimal NCEs were 20, 40, and 50, and the corresponding superimposed spectra were used as the final MS^2 spectra of analytes. For the dd-MS^2 scan mode, it may be difficult to obtain MS^2 spectra with low signal response, resulting in the inability to identify metabolites [33]. Therefore, an inclusion list was added that included the accurate masses of possible metabolites, allowing for purposeful selection of precursor ions for MS^2 fragmentation. In this study, a dynamic exclusion time was set, and the precursor ions with a certain mass-to-charge ratio were excluded within the exclusion time after fragmentation. The purpose of dynamic exclusion time was to obtain as many MS^2 spectra of precursor ions with different mass-to-charge ratios as possible to avoid repeated collection, so as to obtain high-quality MS^2 spectra, and was generally set to the half-peak width [34,35]. In this study, the chromatographic peak shape of each target compound was narrow with a peak width of ≤ 0.2 min, and this might result in the loss of MS^2 spectra of certain precursor ions. Therefore, the dynamic exclusion time was reduced and set to 2 s to obtain more MS^2 spectra of low-abundance precursor ions.

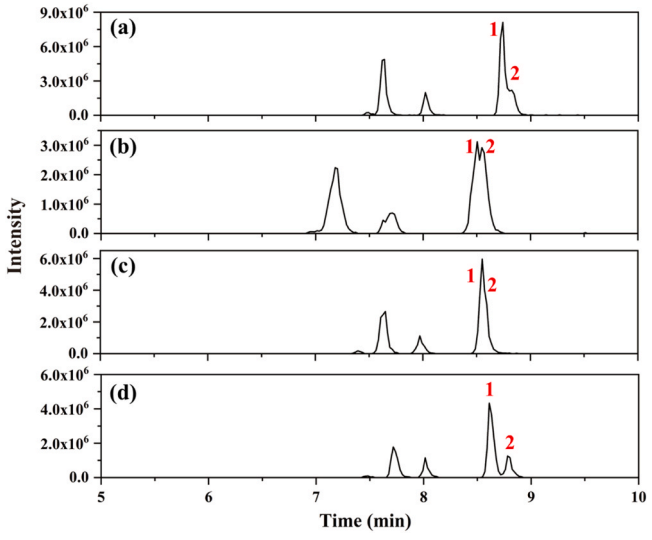

Fig. 2. The extracted ion chromatograms of α-OHFALP (*m/z* 343.0756) in the sample after incubation with FALP through phase I metabolism using different chromatographic columns. (a): Eclipse Plus C18 column; (b): ACUITY UPLC® BEH C18 column; (c): Hypersil GOLD C18 column; (d): ZORBAX RRHD SB C18 column.

3.2. Optimization of incubation conditions

In this study, different control groups were set up to eliminate the interference of other factors on the metabolism of ALP and FALP. For phase I metabolism, three controls were included: no addition of drugs, no addition of liver microsomes, and no addition of NADPH. No metabolites were detected in the first two control groups, proving that liver microsomes were essential for metabolite formation, and only parent drugs were detected without NADPH, indicating its indispensability as a cofactor [36]. Phase II metabolism controls (no addition of UDPGA, no addition of NADPH, and no addition of UDPGA and NADPH) confirmed that UDPGA, as a glucuronic acid donor, was essential in phase II metabolism.

To obtain MS^2 spectra with sufficient signal intensity for reliable metabolite identification, incubation time and liver microsomal enzyme concentration were systematically optimized using rat liver microsomes. Among the detected metabolites, 4-OHALP and 4-OHFALP showed the strongest response signals for ALP and FALP, respectively, and were therefore selected as the objects of the investigation. Since the commercial standards of 4-OHALP and 4-OHFALP were unavailable, semi-quantitative analysis was performed respectively using α-OHALP and α-OHFALP as substitute references. To optimize incubation time, the liver microsomal enzyme concentration and drug concentration were fixed at 0.5 mg mL^{-1} and 0.5 mg L^{-1}, respectively, and metabolite formation was evaluated at incubation times ranging from 5 to 180 min. As shown in Figure S6-**a** and **S6-b**, metabolites levels tended to be stable after 2 h, which was therefore selected as the optimal incubation time. To optimize liver microsomal enzyme concentration, incubations were performed for 2 h with a fixed drug concentration of 0.5 mg L^{-1}, and enzyme concentration levels ranging from 0.1 to 2.5 mg mL^{-1}. As shown in Figure S6-**c** and **S5-d**, the formation of 4-OHFALP stabilized at enzyme concentrations ≥ 1.5 mg mL^{-1}. Considering the economic situation, the enzyme concentration of 1.5 mg mL^{-1} was sufficient to meet the metabolic requirements and was therefore selected for subsequent experiments.

3.3. Identification of metabolites of alprazolam and flualprazolam

To systematically investigate the metabolism of ALP and FALP across multiple species, *in vitro* metabolism studies were conducted using liver microsomes from human, rat, mouse, fish, bovine, sheep, and pig, including phase I and II metabolism. The experiment was conducted according to the optimized incubation conditions mentioned above: the concentration of liver microsomal enzyme was 1.5 mg mL^{-1} and the incubation time was 2 h. In order to increase the diversity and abundance of metabolites for qualitative non-targeted analysis, a relatively high drug concentration of 50 mg L^{-1} was selected, and a blank control (without drugs) was also included. Non-targeted screening was performed and the structures of metabolites of ALP and FALP were putatively deduced based on accurate mass, elemental composition, and MS^2 fragmentation patterns. As a result, a total of 11 metabolites of ALP and FALP respectively were identified, including 7 phase I metabolites and 4 phase II metabolites, with N1, N4, N5, N7, N8 and N11 (ALP) and the 6 corresponding FALP metabolites identified for the first time. The detailed information on metabolites was listed in Tables 1 and 2. The extracted ion chromatograms of ALP, FALP and their metabolites in

Table 1
The detailed information for ALP and its metabolites.

Compound	Formula	Observed (*m/z*)	Theoretical (*m/z*)	Error (ppm)	Composition change	t_R (min)	Source (Ref.)
ALP	$C_{17}H_{13}ClN_4$	309.0904	309.0902	0.65	/	10.35	/
N1	$C_{17}H_{13}ClN_4O$	325.0846	325.0851	−1.54	+ (O)	7.89	Our work
N2	$C_{17}H_{13}ClN_4O$	325.0847	325.0851	−1.23	+ (O)	9.18	[22,23]
N3 (α-OHALP)	$C_{17}H_{13}ClN_4O$	325.0848	325.0851	−0.92	+ (O)	9.41	[22,23]
N4	$C_{17}H_{14}ClN_3O_2$	328.0844	328.0847	−0.91	− (N) + (HO_2)	9.37	Our work
N5	$C_{17}H_{13}ClN_4O_2$	341.0801	341.0800	0.29	+ (O_2)	7.65	Our work
N6	$C_{17}H_{13}ClN_4O_2$	341.0799	341.0800	−0.29	+ (O_2)	8.55	[22,23]
N7	$C_{17}H_{13}ClN_4O_2$	341.0798	341.0800	−0.59	+ (O_2)	9.77	Our work
N8	$C_{23}H_{21}ClN_4O_7$	501.1150	501.1172	−4.39	+ (O) + ($C_6H_8O_6$)	6.33	Our work
N9	$C_{23}H_{21}ClN_4O_7$	501.1157	501.1172	−2.99	+ (O) + ($C_6H_8O_6$)	7.91	[22,23]
N10	$C_{23}H_{21}ClN_4O_7$	501.1179	501.1172	1.40	+ (O) + ($C_6H_8O_6$)	8.10	[22,23]
N11	$C_{23}H_{22}ClN_3O_8$	504.1166	504.1168	−0.40	− (N) + (HO_2) + ($C_6H_8O_6$)	7.95	Our work

Table 2
The detailed information for FALP and its metabolites.

Compound	Formula	Observed (*m/z*)	Theoretical (*m/z*)	Error (ppm)	Composition change	t_R (min)	Source (Ref.)
FALP	$C_{17}H_{12}ClFN_4$	327.0812	327.0807	1.53	/	10.17	/
M1	$C_{17}H_{12}ClFN_4O$	343.0754	343.0756	−0.58	+ (O)	8.71	Our work
M2	$C_{17}H_{12}ClFN_4O$	343.0752	343.0756	−1.17	+ (O)	9.05	[25]
M3 (α-OHFALP)	$C_{17}H_{12}ClFN_4O$	343.0752	343.0756	−1.17	+ (O)	9.16	[25,26]
M4	$C_{17}H_{13}ClFN_3O_2$	346.0750	346.0753	−0.87	− (N) + (HO_2)	9.25	Our work
M5	$C_{17}H_{12}ClFN_4O_2$	359.0709	359.0706	0.84	+ (O_2)	7.94	Our work
M6	$C_{17}H_{12}ClFN_4O_2$	359.0708	359.0706	0.56	+ (O_2)	8.35	[25]
M7	$C_{17}H_{12}ClFN_4O_2$	359.0704	359.0706	−0.56	+ (O_2)	9.55	Our work
M8	$C_{23}H_{20}ClFN_4O_7$	519.1073	519.1077	−0.77	+ (O) + ($C_6H_8O_6$)	6.56	Our work
M9	$C_{23}H_{20}ClFN_4O_7$	519.1071	519.1077	−1.16	+ (O) + ($C_6H_8O_6$)	7.68	[25]
M10	$C_{23}H_{20}ClFN_4O_7$	519.1076	519.1077	−0.19	+ (O) + ($C_6H_8O_6$)	8.07	[25]
M11	$C_{23}H_{21}ClFN_3O_8$	522.1072	522.1074	−0.38	− (N) + (HO_2) + ($C_6H_8O_6$)	7.93	Our work

samples of different species are shown in Figures S7 and S8. Among them, N3 and M3 were confirmed using authentic standards, corresponding to α-OHALP and α-OHFALP respectively. FALP is a new benzodiazepine produced by adding a fluorine atom to ALP, retaining the main chemical structure of ALP. The metabolite screening results revealed a similar metabolic pattern between ALP and FALP. Discussion below focused on FALP as a representative example.

3.3.1. *Identification of phase I metabolites*

The mass spectrometry fragmentation mechanisms of the same type of compounds are usually similar and have similar fragment groups. These fragmentations are analytical phenomena used to deduce chemical structures. In MS/MS analysis of benzodiazepines, fragmentation typically occurs at reactive sites such as the seven-membered ring, hydroxylated carbons, labile heteroatoms, and substituted positions on the benzene ring [37]. The resulting diagnostic fragment ions are crucial for determining the positions of modifications and elucidating metabolite structures. The fragmentation mechanism of FALP was first analyzed. FALP was eluted in liquid chromatography at 10.17 min and the accurate mass of the quasi-molecular ion was *m/z* 327.0807 ($C_{17}H_{12}ClFN_4$) with a mass error of 1.53 ppm. The MS^2 spectrum and deduced fragment ion structures are shown in Fig. 3. Major fragment ions included *m/z* 299.0619 (loss of CH_2N after seven-membered ring opening); *m/z* 292.1119 (loss of Cl); and *m/z* 259.0431 (combined ring opening and triazole loss).

The hydroxylation of FALP is the main phase I metabolic pathway in human body. A study has reported that in the *in vitro* metabolism of human liver microsomes [25], there are corresponding monohydroxylated products α-OHFALP and 4-HOFALP, and a dihydroxylated product α,4-dihydroxy-FALP that are consistent with the ALP metabolic pathway. In this study, three monohydroxylated products (M1-M3, *m/z* 343.0756, $C_{17}H_{12}ClFN_4O$) and three dihydroxylated products (M5-M7, *m/z* 359.0706, $C_{17}H_{12}ClFN_4O_2$) were identified. M4 was identified as a new dihydroxylated products, resulting from loss of a nitrogen atom and conversion of the seven-membered ring of FALP to a six-membered ring (*m/z* 346.0753, $C_{17}H_{13}ClFN_3O_2$). The whole MS^2 spectra and putative fragment ion structures of the phase I metabolites of FALP are shown in Fig. 3.

M3 was confirmed by comparison with the α-OHFALP standard, exhibiting a t_R of 9.16 min in the LC chromatogram (Figure S8). The fragment ion at *m/z* 325.0649 ($C_{17}H_{11}ClFN_4^+$), corresponding to the loss of H_2O (18 Da) from α-OHFALP, indicated that hydroxylation reaction occurred on the carbon of the aliphatic position, as previously reported in the literature [25,38]. This fragmentation pathway can be used as a diagnostic feature to distinguish isomers. The fragment ion of *m/z* 315.0569 ($C_{16}H_{11}ClFN_3O^{\bullet+}$) was generated by the loss of CH_2N from α-OHFALP, which was consistent with the fragmentation characteristic of FALP, and the still existing oxygen atom proved that no hydroxylation reaction occurred on the 4-C position. Therefore, it was determined that a hydroxylation reaction occurred on the 1-C position, corresponding to the metabolite α-OHFALP.

For M2 (t_R = 9.05 min), a highly abundant fragment ion of *m/z* 325.0655 indicated hydroxylation reaction occurred on the aliphatic 4-C position. A fragment ion of *m/z* 315.0810 was observed, but the mass error compared to *m/z* 315.0569 was 76.49 ppm and the absence of *m/z* 315.0569 further indicated hydroxylation reaction occurred on the 4-C position. Finally, it was concluded that M2 was 4-OHFALP.

M1 was a newly identified metabolite in this study. Its fragment ion of *m/z* 308.1069 ($C_{17}H_{13}FN_4O^{\bullet+}$) was generated by the loss of a chlorine atom, which was consistent with the mass spectrometry fragmentation pathway of FALP. The absence of *m/z* 325.0649 indicated that hydroxylation did not occur on the aliphatic 1-C or 4-C positions. The fragment ions of *m/z* 315.0566 and 289.0538 further excluded 4-C and 1-C hydroxylation, respectively. Therefore, it was deduced that the hydroxylation reaction occurred on the carbon of benzene ring, although its specific position on the benzene ring was difficult to accurately determine.

M4 (t_R = 9.25 min) was another newly identified metabolite (Figure S8). Its extracted ion chromatogram showed an impurity peak at 9.05 min, corresponding to the isotope of 4-OHFALP (M2). Despite a

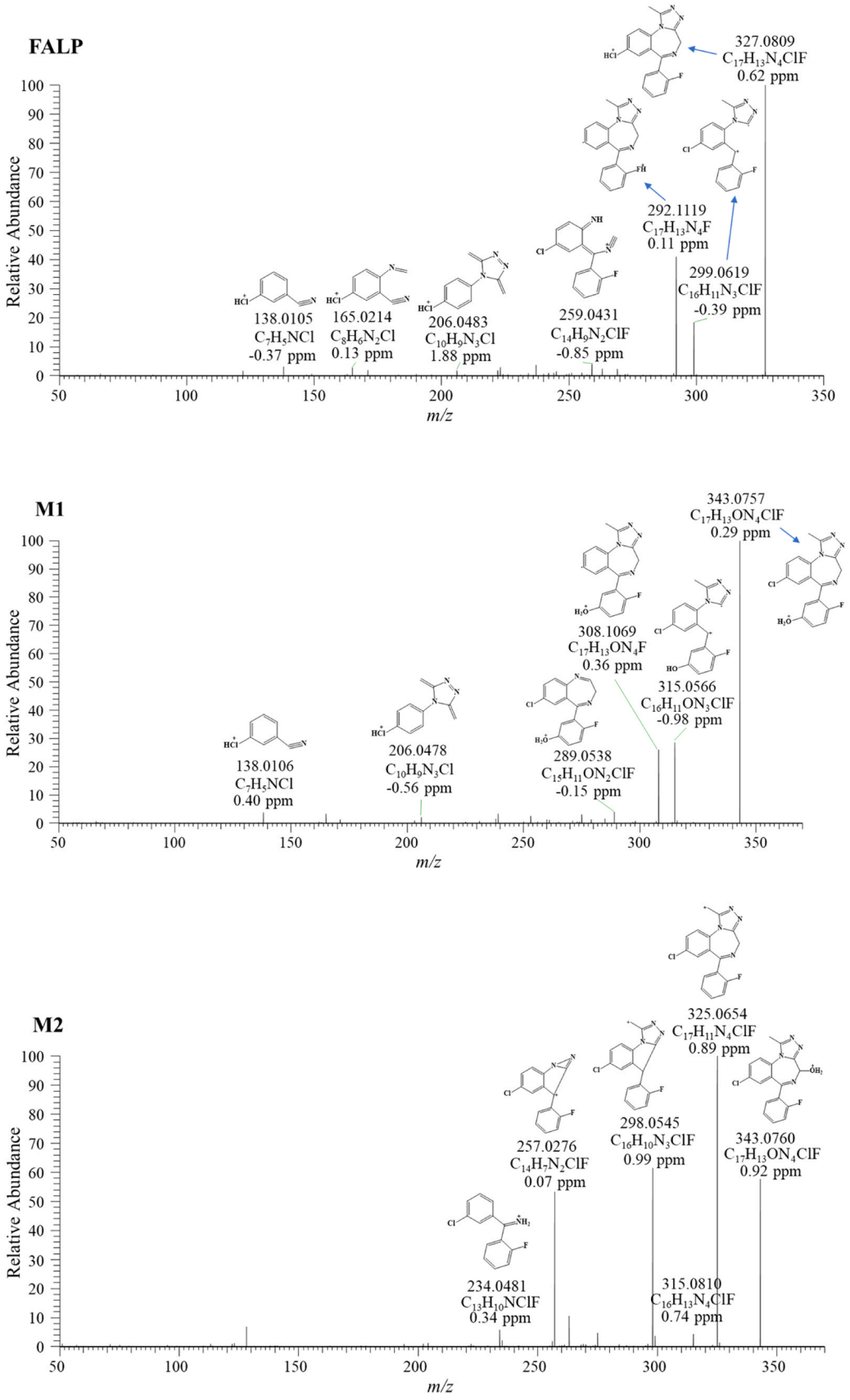

Fig. 3. The MS^2 spectra and putative fragment ion structures of FALP and its phase I metabolites. Metabolites M1, M4, M5, and M7 represent newly identified phase I metabolites in the present study.

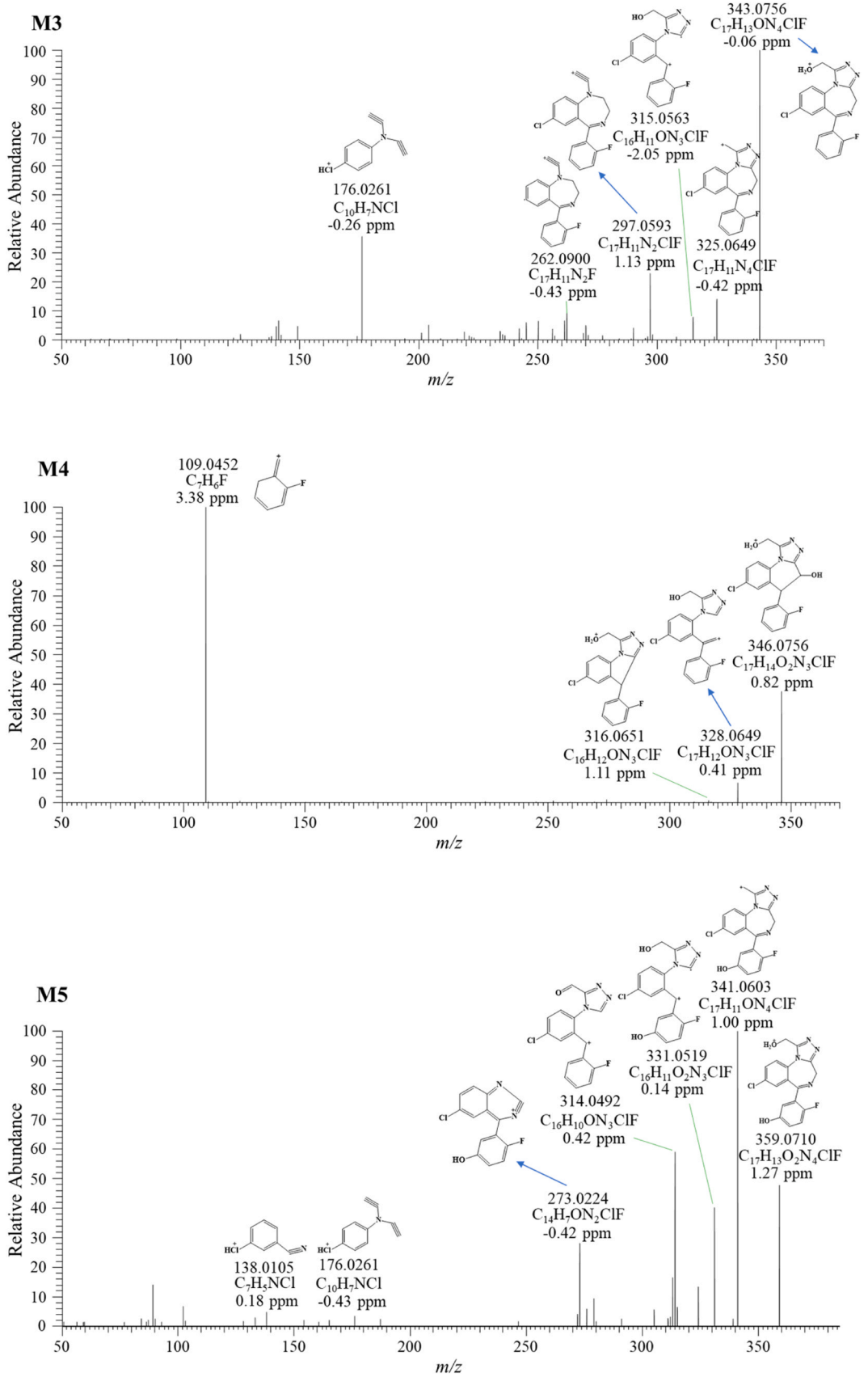

Fig. 3. (*continued*).

small mass difference (2.02 ppm) with the M2 isotope (*m/z* 346.0760), M4 was effectively separated by LC. M4 had relatively abundant fragment ions of *m/z* 328.0649 and *m/z* 109.0452, of which *m/z* 328.0649 was produced by the loss of a molecule of water from M4,

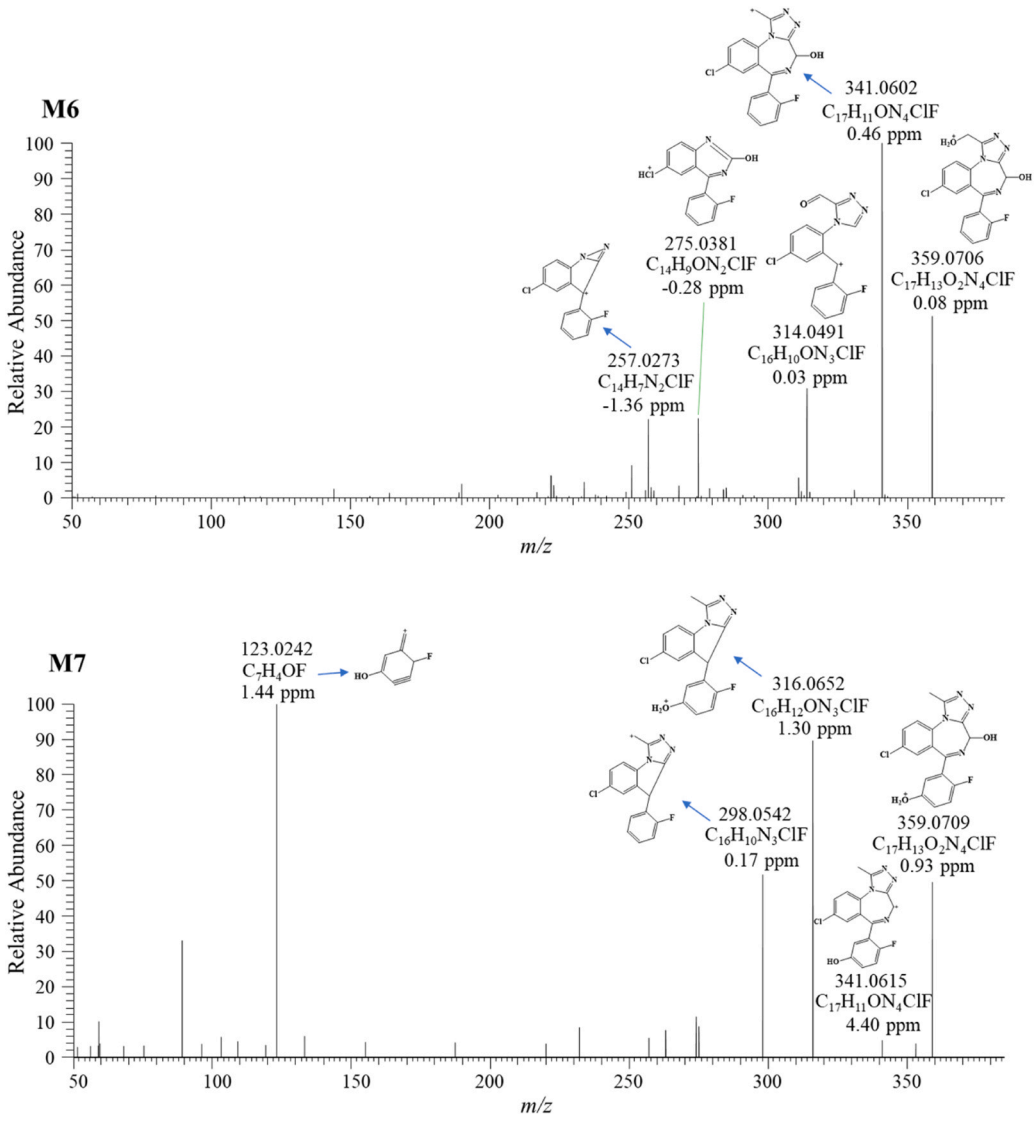

Fig. 3. (*continued*).

which was a characteristic fragment of hydroxylation reaction occurring on the carbon of the aliphatic position. The fragment ion of *m/z* 109.0452 was a benzene ring with a fluorine atom. Therefore, the tentative structure of M4 was deduced as shown in Fig. 3.

Dihydroxylated products M5, M6 and M7 eluted at 7.65, 8.55 and 9.77 min, respectively. According to their extracted ion chromatogram (Figure S8), multiple chromatographic peaks with different t_R suggested positional isomers due to hydroxylation reaction on the benzene ring. For M6, a highly abundant fragment ion of *m/z* 341.0602 was found, which was produced by the loss of a molecule of water. In addition, it was inferred from the fragment ion of *m/z* 314.0491 that one of the hydroxylation reactions occurred on the 1-C or the benzene ring position. The presence of the fragment ion of *m/z* 275.0381 indicated that one of the hydroxylation reactions occurred on the 4-C or benzene ring position. Although its fragment ions might be common to multiple structures and were not obviously characterized, there were no characteristic fragment ions for hydroxylation reaction on the benzene ring. Furthermore, according to the monohydroxylation reaction of FALP, it was easier to occur on the 1-C and 4-C positions, and M6 had a strong signal intensity in the extracted ion chromatogram. Therefore, M6 was reasonably deduced to be α,4-dihydroxy-FALP, which was also a metabolite reported in the literature [25].

M5 and M7 were newly identified metabolites, too. For M5, the fragment ion of *m/z* 341.0603 was observed, which was produced by M5 losing a molecule of water. The fragment ion of *m/z* 331.0519 ($C_{16}H_{11}ClFN_3O_2^{\bullet+}$) was produced by the loss of CH_2N from M5, and there were still two oxygen atoms in its molecular formula, proving that hydroxylation reaction did not occur on the 4-C position. The fragment ion of *m/z* 273.0224 preliminarily indicated the presence of a phenolic hydroxyl group on the benzene ring. In summary, the hydroxylation reactions of M5 occurred on the 1-C and the benzene ring positions. For M7, a relatively abundant fragment ion of *m/z* 123.0242 ($C_7H_4OF^+$) indicated hydroxylation on the benzene ring. There was a low-abundance fragment ion of *m/z* 341.0615, which was produced by the loss of a molecule of water from M7. Additionally, the fragment ions at *m/z* 298.042 and *m/z* 316.0652 in M7 were consistent with those of other metabolites, such as M2 and M4, respectively. However, there were no characteristic for judging the position of hydroxylation. Therefore, M7 was tentatively deduced as a dihydroxylated product of FALP at the 4-C and benzene ring positions.

3.3.2. *Identification of phase II metabolites*

Phase II metabolism of drugs primarily involves conjugation reactions, in which drugs or their phase I metabolites are coupled with endogenous substances (such as glucuronic acid, glycine, sulfate, etc.), or undergo methylation or acetylation reactions catalyzed by specific

enzymes. These conjugation reactions typically yield inactive metabolites, serving as a detoxification mechanism [39]. Among them, glucuronidated products are the main phase II metabolites of drugs [40], so a UGT incubation system was used to investigate phase II metabolites in this study. The results of phase II metabolism of FALP indicated that it primarily proceeded via glucuronidation of its phase I hydroxylated metabolites. Four glucuronide conjugates were formed through enzyme-mediated coupling between glucuronic acid and hydroxyl groups, as shown in Figure S9. The MS^2 spectra and putative fragment ion structures of the phase II metabolites of FALP are shown in Figure S10. In their MS^2 spectra, all fragment ions, except for the quasi-molecular ion peak, were identical to those of the corresponding phase I hydroxylated metabolites, with comparable relative abundances. The accurate mass of metabolites M8, M9 and M10 was *m/z* 519.1077 ($C_{23}H_{20}ClFN_4O_7$), indicating the addition of one oxygen atom and $C_6H_8O_6$ compared with the parent drug FALP. Their MS^2 spectra, apart from the quasi-molecular ion peaks, were consistent with those of M1, M3 and M2 respectively. The accurate mass of metabolite M11 was *m/z* 522.1074 ($C_{23}H_{21}ClFN_3O_8$), corresponding to the addition of a $C_6H_8O_6$ to M4, and the fragment ions in its MS^2 spectrum were consistent with those of M4.

The results showed that the phase I metabolic pathways of ALP and FALP were mainly based on the hydroxylation reaction, and the phase II metabolic pathways were based on the glucuronidation reaction of phase I metabolites. The metabolic patterns of ALP and FALP were similar, and the deduced structures of their metabolites and the potential metabolic pathways are shown in Fig. 4. New benzodiazepines are generally produced with slight modifications of known drugs. Therefore, the structures of new benzodiazepines and metabolites was preliminarily deduced based on existing research foundations.

3.4. Comparison of in vitro metabolism in different species

Although ALP is used in both humans and animals, the lack of metabolic studies in different animals may affect the scientific basis for setting residue markers in food. FALP is a new benzodiazepine that adds a fluorine atom to ALP. In this study, the *in vitro* metabolism differences of ALP and FALP were compared in humans, model animals, aquatic animals and livestock animals, such as human, rat, mouse, fish, bovine, sheep and pig. Their extracted ion chromatograms of metabolites are shown in Figures S7 and S8, respectively. To facilitate a clearer comparison of the number of metabolites detected for each compound across different species, Tables S1 and S2 systematically summarize the presence or absence of metabolites derived from ALP and FALP, respectively, across all investigated species, providing an intuitive overview of metabolite distribution and detection numbers and enabling a comprehensive comparison of interspecies metabolic profiles.

The newly identified metabolites N4 and M4, along with their corresponding phase II metabolites, exhibited strong signal responses and were detected in all species. Species-specific differences were observed in the dominant metabolic pathways of ALP and FALP. In humans and mice, both compounds exhibited similar metabolic profiles, with 9 and 7 metabolites identified, respectively. The 4-hydroxylation and α-hydroxylation represented the major metabolic pathways, among which the 4-hydroxylated products showed the highest signal intensity. This is consistent with previous studies reporting that ALP is primarily metabolized to 4-OHALP and α-OHALP in the human body, with 4-OHALP exhibiting higher plasma concentrations following administration [41–43]. In contrast, in edible animals such as bovine, sheep, and pig, the metabolic profiles were relatively similar to those observed in rats, with 4-hydroxylated products as the predominant metabolites and limited formation of α-hydroxylated products. Notably, although the overall number of detected metabolites in fish was lower, the dominant metabolic pathway was likewise characterized by 4-hydroxylation. This difference in major oxidative pathways indicates species-dependent enzyme selectivity, potentially reflecting differences in cytochrome P450 isoform expression or activity [28]. However, the standard method for the detection of benzodiazepines in food exported from China issued in 2019 only included ALP and α-OHALP [24]. In addition, hydroxylation on the benzene ring, along with its corresponding dihydroxylated and phase II conjugated metabolites, was mainly observed in rats and livestock species (e.g., M1, M5, M7, and M8), further highlighting interspecies variation in metabolic pathways.

These species-specific metabolic preferences may have important implications for pharmacokinetics and toxicity. From a food safety perspective, the identification of abundant other hydroxylated metabolites in edible animals suggests that current residue monitoring strategies focusing primarily on ALP and α-OHALP may underestimate total benzodiazepine-related residues. Therefore, incorporating species-specific metabolic information is essential for a more accurate assessment of residue markers and potential toxicological risks.

3.5. Toxicity prediction of drugs and their metabolites

To further understand the toxicity of drug metabolites, a preliminary assessment of the toxicity of ALP, FALP and their metabolites was performed using two complementary quantitative structure activity relationship (QSAR) tools: ECOSAR and TEST. The purpose of this toxicity prediction was to provide an initial indication of the potential toxicological relevance of the identified metabolites and to serve as a reference for subsequent targeted toxicological investigations. ECOSAR predicts acute and chronic toxicity toward aquatic organisms based on linear mathematical relationship between octanol-water partition coefficient (Log K_{ow}) and toxicity of compound, providing insight into potential environmental risks. TEST integrates multiple QSAR models and algorithms to predict a wider range of endpoints, including physical, chemical, health, and ecotoxicological effects. The use of both tools enabled complementary evaluation of potential ecological and developmental risks, cross-validation of predictions, and identification of structure-toxicity relationships among metabolites with different hydroxylation patterns. Phase II metabolism is generally a detoxification pathway that produces highly water-soluble inactive products through conjugation reactions [39]. Therefore, the toxicity assessment primarily focused on phase I metabolites. The predicted toxicity of ALP, FALP and their phase I metabolites for different species endpoints is summarized in Tables S3 and S4 respectively. The results showed that ALP, FALP and their metabolites had similar toxicity prediction results due to the similarity in chemical structure. The following discussion used FALP as a representative example.

The results using ECOSAR showed that the overall toxicity of the metabolites was slightly less than that of FALP. In general, hydroxylated products are more water-soluble, and this toxicity prediction result is consistent with the trend that drugs are more easily converted into metabolites that are more polar and relatively less toxic. A previous study reported the use of median lethal concentration (LC_{50}) or median effective dose (EC_{50}) at 1, 10, and 100 mg L^{-1} to determine various toxicity levels of the acute and chronic toxicity of compounds to fish and *Green algae* [44]. In this present work, the predicted toxicity of FALP and its metabolites showed moderate to low toxicity toward *Daphnid* and *Green algae*. Predicted toxicity to fish showed that the dihydroxylated products of FALP are no-harmful ($LC_{50} > 100$ mg L^{-1}). The results using TEST showed that the metabolites were less toxic to *Daphnia magna* than FALP. For *Tetrahymena pyriformis*, M1, M5 and M7 were more toxic than FALP, while the others were less toxic than the parent drug. However, the toxicity results of the *Fathead minnow* showed that most of the metabolites were more toxic than FALP, except for two metabolites, M3 and M4, which were slightly less toxic than the parent drug. In addition, except for FALP and one of the newly identified metabolites M4, all others showed developmental toxicity. The predicted ecotoxicity and developmental toxicity by TEST indicated that some metabolites exhibited stronger toxic effects than the parent drug, providing a reference for future toxicological studies.

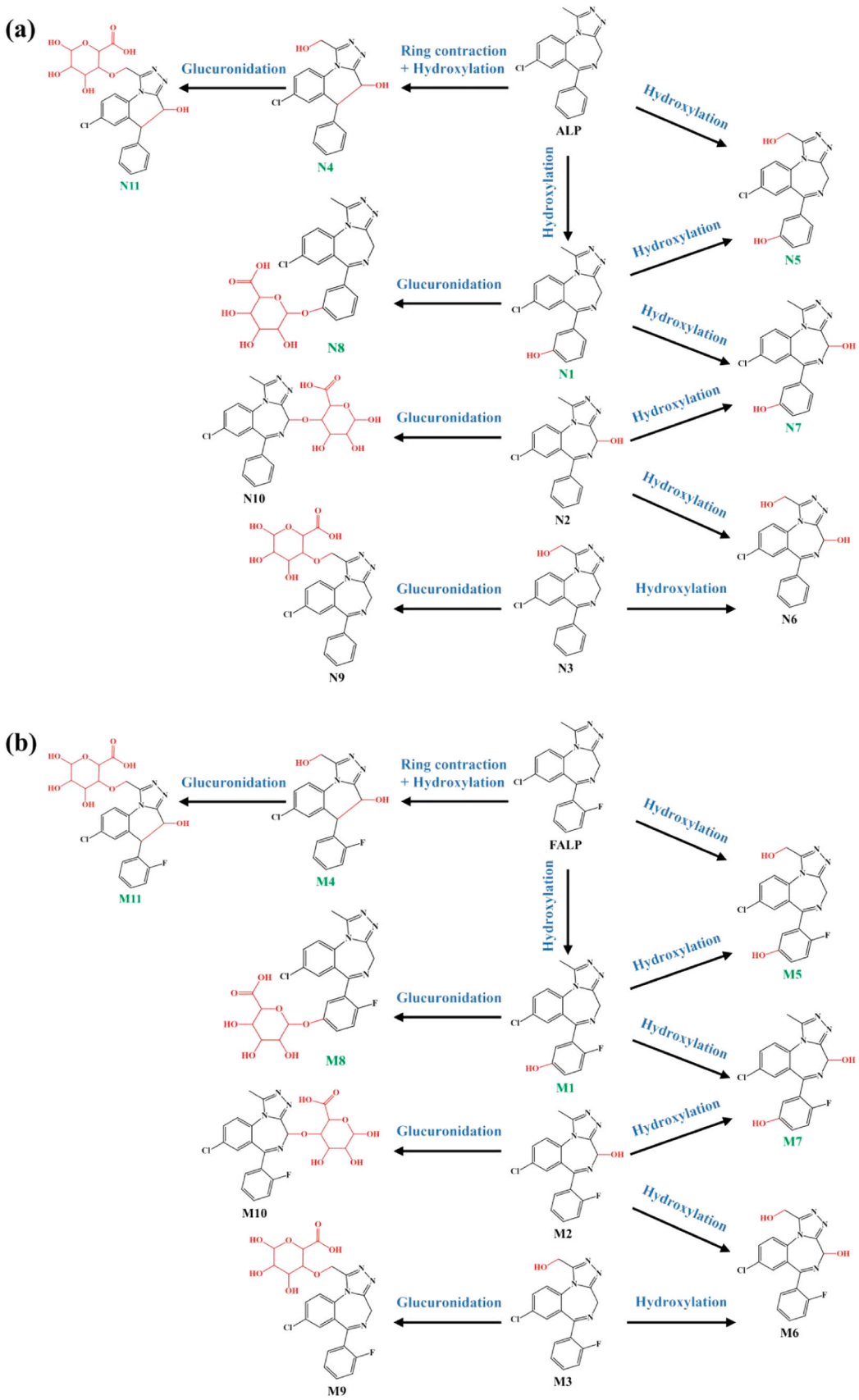

Fig. 4. The potential metabolic pathways of ALP (a) and FALP (b). Newly identified metabolites in this study are labeled in green symbols.

In addition, clear structure-toxicity relationships were observed among different hydroxylation patterns. Among the monohydroxylated metabolites, the newly identified benzene-ring hydroxylated product (M1) exhibited higher predicted toxicity than both α-hydroxylated and 4-hydroxylated metabolites across several endpoints. Similarly, among the dihydroxylated metabolites, compounds retaining a hydroxyl group on the benzene ring (e.g., M5 and M7) showed higher predicted toxicity than the α,4-dihydroxylated metabolite (M6), indicating that benzene-ring hydroxylation may play a critical role in enhancing toxicological potential. By comparison, α-hydroxylation and 4-hydroxylation pathways resulted in metabolites with broadly comparable predicted toxicity profiles, and both types of metabolites were associated with potential developmental toxicity. These findings suggest that while hydroxylation is commonly considered a detoxification step, the specific site of hydroxylation strongly influences toxicological outcomes, particularly for benzene-ring hydroxylation, which may confer increased biological reactivity.

From a forensic toxicology standpoint, these findings are particularly relevant given the increasing detection of FALP in illicit drug use cases [19]. Several hydroxylated and glucuronidated metabolites identified in this study were partially consistent with biomarkers reported in previous literature reports, supporting their utility for confirming FALP exposure when the parent compound is present at trace levels or even absent [25,26]. Therefore, integrating species-specific metabolic information with toxicity prediction not only improves understanding of pharmacokinetic and toxicological behavior but also enhances the interpretation of forensic and food safety monitoring data.

4. Conclusion

FALP, a new psychoactive substance and structural analog of ALP, has emerged as a widely abused illicit benzodiazepine with increasing global prevalence but limited understanding of its metabolic behavior across species. In this study, the phase I and II metabolism of ALP and FALP was investigated using the *in vitro* liver microsome system from multiple species. Non-targeted screening identified 11 metabolites for each drug, including 7 phase I and 4 phase II metabolites. In addition to previously reported 4-hydroxylated, α-hydroxylated and α,4-dihydroxylated products, new benzene-ring hydroxylated products and their corresponding dihydroxylated and phase II metabolites were identified, expanding the known metabolic pathways. Phase I metabolism was dominated by hydroxylation reactions, whereas phase II metabolism primarily involved glucuronidation of phase I metabolites. By comparing interspecies metabolic differences of drugs, it was found that 4-hydroxylated and α-hydroxylated products predominated in humans, while 4-hydroxylated metabolites dominated in edible animals, providing theoretical support for the selection of residue markers. Toxicity predictions further indicated that some metabolites, particularly the newly identified benzene-ring hydroxylated products, may exhibit higher ecotoxicological or developmental risks than the parent drugs and the currently monitored residue markers.

It should be noted that this study employed a non-targeted HRMS strategy with optimized analytical conditions and semi-quantitative analysis due to the lack of certified authentic standards. Although non-targeted screening may be prone to false-positive signals and limited sensitivity toward low-abundance metabolites especially towards phase II metabolites, all metabolites reported here were stringently validated based on high-quality MS/MS spectra, accurate mass measurements, and biologically feasible metabolic pathways. Candidate metabolites lacking sufficient signal intensity or confirmatory fragmentation were excluded to ensure identification reliability. Future studies incorporating targeted quantitative analysis with authentic standards are warranted to enable absolute quantification and to further refine the toxicological relevance of key metabolites. Overall, this study provides a scientific basis for the rational monitoring, environmental risk assessment, and management of benzodiazepine residues in animal-derived foods and ecosystems.

Environmental implication

Residues of flualprazolam and alprazolam in animal-derived foods and environmental waters can transform into previously unreported toxic metabolites, which may further bioaccumulate and pose risks to humans and ecosystems. This study elucidates species-specific biotransformation by identifying new metabolites and comparing their interspecies metabolic pathways, thereby providing a scientific basis for residue monitoring, environmental risk assessment, and food safety management.

CRediT authorship contribution statement

Chun-xiang Xu: Supervision, Resources, Project administration. **Jun-qin Qiao:** Validation, Investigation, Data curation. **Hong-zhen Lian:** Writing – review & editing, Supervision, Resources, Project administration, Funding acquisition, Conceptualization. **Hui Lin:** Software, Resources, Investigation. **Jinxia Dai:** Writing – original draft, Visualization, Methodology, Investigation, Formal analysis, Data curation.

Funding

This work was supported by the National Natural Science Foundation of China [grant numbers 22176085, 21874065]; and the National Key R&D Program of China [grant number 2019YFC1605400].

Declaration of Competing Interest

The authors declare that they have no known competing financial interests or personal relationships that could have appeared to influence the work reported in this paper.

Appendix A. Supporting information

Supplementary data associated with this article can be found in the online version at doi:10.1016/j.jhazmat.2026.141380.

Data availability

Data will be made available on request.

References

[1] Howard, P., Twycross, R., Shuster, J., Mihalyo, M., Wilcock, A., 2014. Benzodiazepines. J Pain Symptom Manag 47, 955–964. https://doi.org/10.1016/j.jpainsymman.2014.03.001.
[2] Yin, X., Guo, C., Teng, Y., Xu, J., 2019. Development and application of the analytical method for illicit drugs and metabolites in fish tissues. Chemosphere 233, 532–541. https://doi.org/10.1016/j.chemosphere.2019.06.018.
[3] Kuang, H., Gan, B., Guo, L., Aguilar, Z.P., Xu, H., 2016. Determination of benzodiazepines in beef by magnetic solid phase extraction and high-performance liquid chromatography-tandem mass spectrometry. Anal Lett 49, 499–510. https://doi.org/10.1080/00032719.2015.1076830.
[4] McHugh, R.K., Votaw, V.R., Trapani, E.W., McCarthy, M.D., 2023. Prevalence and correlates of the misuse of z-drugs and benzodiazepines in the National Survey on Drug Use and Health. Front Psychiatry 14, 1129447. https://doi.org/10.3389/fpsyt.2023.1129447.
[5] Gupta, N., Thakur, R.S., Patel, D.K., 2023. Detection, quantification and degradation kinetic for five benzodiazepines using VAUS-ME-SFO/LC-MS/MS method for water, alcoholic and non-alcoholic beverages. Talanta 260, 124572. https://doi.org/10.1016/j.talanta.2023.124572.
[6] Vincenti, F., Montesano, C., Babino, P., Carboni, S., Napoletano, S., De Sangro, G., Di Rosa, F., Gregori, A., Curini, R., Sergi, M., 2021. Finding evidence at a crime scene: sensitive determination of benzodiazepine residues in drink and food paraphernalia by HPLC-HRMS/MS. Forensic Chem 23, 100327. https://doi.org/10.1016/j.forc.2021.100327.
[7] Wang, J., Wang, Y., Pan, Y., Feng, L., Chen, D., Liu, Z., Peng, D., Yuan, Z., 2016. Preparation of a broadly specific monoclonal antibody-based indirect competitive

ELISA for the detection of benzodiazepines in edible animal tissues and feed. Food Anal Method 9, 3407–3419. https://doi.org/10.1007/s12161-016-0528-0.
[8] Li, J., Zhang, J., Liu, H., Wu, L., 2016. A comparative study of primary secondary amino (PSA) and multi-walled carbon nanotubes (MWCNTs) as QuEChERS absorbents for the rapid determination of diazepam and its major metabolites in fish samples by high-performance liquid chromatography-electrospray ionization-tandem mass spectrometry. J Sci Food Agric 96, 555–560. https://doi.org/10.1002/jsfa.7123.
[9] Wang, Z., Wang, W., Yang, F., 2023. Species-specific bioaccumulation and risk prioritization of psychoactive substances in cultured fish. Chemosphere 325, 138440. https://doi.org/10.1016/j.chemosphere.2023.138440.
[10] Golbaz, S., Zamanzadeh, M., Yaghmaeian, K., Nabizadeh, R., Rastkari, N., Esfahani, H., 2023. Occurrence and removal of psychiatric pharmaceuticals in the Tehran South Municipal Wastewater Treatment Plant. Environ Sci Pollut Res 30, 27041–27055. https://doi.org/10.1007/s11356-022-23667-5.
[11] Mohamadpour, F., Mohamadpour, F., 2024. Photodegradation of six selected antipsychiatric drugs; carbamazepine, sertraline, amisulpride, amitriptyline, diazepam, and alprazolam in environment: efficiency, pathway, and mechanism-a review. Sustain Environ Res 34 (1), 8. https://doi.org/10.1186/s42834-024-00214-0.
[12] Matey, J.M., Zapata, F., Menéndez-Quintanal, L.M., Montalvo, G., García-Ruiz, C., 2023. Identification of new psychoactive substances and their metabolites using non-targeted detection with high-resolution mass spectrometry through diagnosing fragment ions/neutral loss analysis. Talanta 265, 124816. https://doi.org/10.1016/j.talanta.2023.124816.
[13] Hikin, L.J., Coombes, G., Rice-Davies, K., Couchman, L., Smith, P.R., Morley, S.R., 2024. Post mortem blood bromazolam concentrations and co-findings in 96 coronial cases within England and Wales. Forensic Sci Int 354, 111891. https://doi.org/10.1016/j.forsciint.2023.111891.
[14] Edinoff, A.N., Nix, C.A., Odisho, A.S., Babin, C.P., Derouen, A.G., Lutfallah, S.C., Cornett, E.M., Murnane, K.S., Kaye, A.M., Kaye, A.D., 2022. Novel designer benzodiazepines: comprehensive review of evolving clinical and adverse effects. Neurol Int 14, 648–663. https://doi.org/10.3390/neurolint14030053.
[15] Brunetti, P., Giorgetti, R., Tagliabracci, A., Huestis, M., Busardò, F., 2021. Designer benzodiazepines: a review of toxicology and public health risks. Pharmaceuticals 14, 560. https://doi.org/10.3390/ph14060560.
[16] Hauck, T.S., Rochon, S., Bahra, P., Selby, P., 2022. Outpatient treatment of chronic designer benzodiazepine use: a case report. J Addict Med 16, e137–e139. https://doi.org/10.1097/ADM.0000000000000857.
[17] Corkery, J.M., Guirguis, A., Chiappini, S., Martinotti, G., Schifano, F., 2022. Alprazolam-related deaths in Scotland, 2004-2020. J Psychopharmacol 36, 1020–1035. https://doi.org/10.1177/02698811221104065.
[18] Syrjanen, R., Greene, S.L., Weber, C., Smith, J.L., Hodgson, S.E., Abouchedid, R., Gerostamoulos, D., Maplesden, J., Knott, J., Hollerer, H., Rotella, J., Graudins, A., Schumann, J.L., 2023. Characteristics and time course of benzodiazepine-type new psychoactive substance detections in Australia: results from the Emerging Drugs Network of Australia-Victoria project 2020-2022. Int J Drug Policy 122, 104245. https://doi.org/10.1016/j.drugpo.2023.104245.
[19] Kriikku, P., Rasanen, I., Ojanperä, I., Thelander, G., Kronstrand, R., Vikingsson, S., 2020. Femoral blood concentrations of flualprazolam in 33 postmortem cases. Forensic Sci Int 307, 110101. https://doi.org/10.1016/j.forsciint.2019.110101.
[20] Bollinger, K., Weimer, B., Heller, D., Bynum, N., Grabenauer, M., Pressley, D., Smiley-McDonald, H., 2021. Benzodiazepines reported in NFLIS-Drug, 2015–2018. Forensic Sci Int Synerg 3, 100138. https://doi.org/10.1016/j.fsisyn.2021.100138.
[21] Ministry of Public Security of the People's Republic of China, 2021. Announc Incl 18 Subst Incl Synth cannabinoids fluoketamine Suppl Cat Control NonMed Narc Drugs Psychotr Subst. ⟨https://www.mps.gov.cn/n6557558/c7881251/content.html⟩ (accessed 13 March 2024).
[22] Hirota, N., Ito, K., Iwatsubo, T., Green, C.E., Tyson, C.A., Shimada, N., Suzuki, H., Sugiyama, Y., 2001. *In vitro/in vivo* scaling of alprazolam metabolism by CYP3A4 and CYP3A5 in humans. Biopharm Drug Dispos 22, 53–71. https://doi.org/10.1002/bdd.261.
[23] Tanaka, E., Nakamura, T., Terada, M., Shinozuka, T., Honda, K., 2007. Metabolic interaction between ethanol, high-dose alprazolam and its two main metabolites using human liver microsomes *in vitro*. J Forensic Leg Med 14, 348–351. https://doi.org/10.1016/j.jflm.2006.11.004.
[24] 2019. Industry Standards for Entry Exit Inspection and Quarantine of the People's Republic of China, Determination of benzodiazepines residues in foodstuffs for export-LC-MS/MS method, SN/T 3847-2019, 2019.
[25] Wagmann, L., Manier, S.K., Bambauer, T.P., Felske, C., Eckstein, N., Flockerzi, V., Meyer, M.R., 2020. Toxicokinetics and analytical toxicology of flualprazolam: metabolic fate, isozyme mapping, human plasma concentration and main urinary excretion products. J Anal Toxicol 44, 549–558. https://doi.org/10.1093/jat/bkaa019.
[26] Ling, J., Zhang, W., Yan, X., Liu, W., Wang, Y., Ding, Y., 2022. Sensitive detection and primary metabolism analysis of flualprazolam in blood. J Forensic Leg Med 90, 102388. https://doi.org/10.1016/j.jflm.2022.102388.
[27] Wei, G., Yan, C., Zou, L., Liu, Y., Yang, L., 2025. Species differences in microsomal metabolism of hydroxychloroquine. Toxicol Vitr 107, 106063. https://doi.org/10.1016/j.tiv.2025.106063.
[28] Wu, Q., Hu, Y., Wang, C., Wei, W., Gui, L., Zeng, W., Liu, C., Jia, W., Miao, J., Lan, K., 2022. Reevaluate in vitro CYP3A index reactions of benzodiazepines and steroids between humans and dogs. Drug Metab Dispos 50, 741–749. https://doi.org/10.1124/dmd.122.000864.
[29] Wu, W., Xia, B., Liu, S., Huang, X., Guo, T., Shi, P., Chen, X., Xiao, Q., Zhang, M., Wan, Y., Zhou, Y., 2025. High-throughput screening of new psychoactive substances and related compounds in food by UHPLC-Q/Orbitrap. Food Chem 476, 143278. https://doi.org/10.1016/j.foodchem.2025.143278.
[30] Pandey, A., Yahavi, C., Bhateria, M., Khan, A.R., Singh, S.P., 2025. Identification of Beauvericin metabolites using rat and human liver microsomes and in vivo urinary excretion study in rats for biomonitoring application. Toxicol Vitr 103, 105969. https://doi.org/10.1016/j.tiv.2024.105969.
[31] Dubreil, E., Sczubelek, L., Burkina, V., Zlabek, V., Sakalli, S., Zamaratskaia, G., Hurtaud-Pessel, D., Verdon, E., 2020. *In vitro* investigations of the metabolism of Victoria pure blue BO dye to identify main metabolites for food control in fish. Chemosphere 238, 124538. https://doi.org/10.1016/j.chemosphere.2019.124538.
[32] Sultan, A., Hindrichs, C., Cisneros, K.V., Weaver, C.J., Faux, L.R., Agarwal, V., James, M.O., 2022. Hepatic demethylation of methoxy-bromodiphenyl ethers and conjugation of the resulting hydroxy-bromodiphenyl ethers in a marine fish, the red snapper, Lutjanus campechanus, and a freshwater fish, the channel catfish, *Ictalurus punctatus*. Chemosphere 286, 131620. https://doi.org/10.1016/j.chemosphere.2021.131620.
[33] Turnipseed, S.B., Storey, J.M., Lohne, J.J., Andersen, W.C., Burger, R., Johnson, A. S., Madson, M.R., 2017. Wide-scope screening method for multiclass veterinary drug residues in fish, shrimp, and eel using liquid chromatography-quadrupole high-resolution mass spectrometry. J Agric Food Chem 65, 7252–7267. https://doi.org/10.1021/acs.jafc.6b04717.
[34] Assress, H.A., Ferruzzi, M.G., Lan, R.S., 2023. Optimization of mass spectrometric parameters in data dependent acquisition for untargeted metabolomics on the basis of putative assignments. J Am Soc Mass Spectrom 34, 1621–1631. https://doi.org/10.1021/jasms.3c00084.
[35] Tian, Y., Ma, B., Liu, C., Zhao, X., Yu, S., Li, Y., Tian, S., Pei, H., Wang, Z., Zuo, Z., Wang, Z., 2022. Integrated solid-phase extraction, ultra-high-performance liquid chromatography-quadrupole-orbitrap high-resolution mass spectrometry, and multidimensional data-mining techniques to unravel the metabolic network of dehydrocostus lactone in rats. Molecules 27, 7688. https://doi.org/10.3390/molecules27227688.
[36] Xu, D., Zhang, W., Li, J., Wang, J., Qin, S., Lu, J., 2019. Analysis of AMB-FUBINACA biotransformation pathways in human liver microsome and zebrafish systems by liquid chromatography-high resolution mass spectrometry. Front Chem 7, 1–9. https://doi.org/10.3389/fchem.2019.00240.
[37] Wagmann, L., Manier, S.K., Felske, C., Gampfer, T.M., Richter, M.J., Eckstein, N., Meyer, M.R., 2021. Flubromazolam-derived designer benzodiazepines: toxicokinetics and analytical toxicology of clobromazolam and bromazolam. J Anal Toxicol 45, 1014–1027. https://doi.org/10.1093/jat/bkaa161.
[38] Niessen, W.M.A., Correa, C.R.A., 2017. Interpretation of MS-MS mass spectra of drugs and pesticides. John Wiley & Sons, Hoboken, New Jersey.
[39] Chhatrapati Bisen, A., Nashik Sanap, S., Agrawal, S., Biswas, A., Sankar Bhatta, R., 2023. Chemical metabolite synthesis and profiling: mimicking in vivo biotransformation reactions. Bioorg Chem 139, 106722. https://doi.org/10.1016/j.bioorg.2023.106722.
[40] Grapp, M., Kaufmann, C., Schwelm, H.M., Neukamm, M.A., 2023. Toxicological investigation of a case series involving the synthetic cathinone α-pyrrolidinohexiophenone (α-PHP) and identification of phase I and II metabolites in human urine. J Anal Toxicol 47, 162–174. https://doi.org/10.1093/jat/bkac057.
[41] Allqvist, A., Wennerholm, A., Svensson, J., Mirghani, R.A., 2005. Simultaneous quantification of alprazolam, 4- and α-hydroxyalprazolam in plasma samples using liquid chromatography mass spectrometry. J Chromatogr B 814, 127–131. https://doi.org/10.1016/j.jchromb.2004.10.012.
[42] Wennerholm, A., Allqvist, A., Svensson, J., Gustafsson, L.L., Mirghani, R.A., Bertilsson, L., 2005. Alprazolam as a probe for CYP3A using a single blood sample: pharmacokinetics of parent drug, and of α- and 4-hydroxy metabolites in healthy subjects. Eur J Clin Pharm 61, 113–118. https://doi.org/10.1007/s00228-004-0861-x.
[43] Charpentier, K.P., Von Moltke, L.L., Poku, J.W., Harmatz, J.S., Shader, R.I., Greenblatt, D.J., 1997. Alprazolam hydroxylation by mouse liver microsomes in vitro: the effect of age and phenobarbital induction. Biopharm Drug Dispos 18, 139–149 https://doi.org/10.1002/(SICI)1099-081X(199703)18:2<139::AID-BDD7>3.0.CO;2-Z.
[44] Fang, L., Xu, L., Zhang, N., Shi, Q., Shi, T., Ma, X., Wu, X., Li, Q.X., Hua, R., 2021. Enantioselective degradation of the organophosphorus insecticide isocarbophos in Cupriavidus nantongensis X1^{T}: characteristics, enantioselective regulation, degradation pathways, and toxicity assessment. J Hazard Mater 417, 126024. https://doi.org/10.1016/j.jhazmat.2021.126024.